A Hybrid RF and Vibration Energy Harvester for Wearable Devices

Son Nguyen, Rajeevan Amirtharajah
Department of Electrical and Computer Engineering
University of California, Davis, CA, USA
sohngunen@ucdavis.edu, ramirtha@ucdavis.edu

***Abstract*— This paper describes a hybrid radio frequency (RF) and piezoelectric thin film polyvinylidene fluoride (PVDF) vibration energy harvester for wearable devices. By exploiting the impedance characteristics of parasitic capacitances and discrete inductors, the proposed harvester not only scavenges 15 Hz vibration energy but also works as a 915 MHz flexible silver-ink RF dipole antenna. In addition, an interface circuit including a 6-stage Dickson RF-to-DC converter and a diode bridge rectifier to convert the RF and vibration outputs of the hybrid harvester into DC signals to power resistive loads is evaluated. A maximum DC output power of 20.9 µW, when using the RF to DC converter and -8 dBm input RF power, is achieved at 36% of the open-circuit output voltage while the DC power harvested from 3 g vibration excitation reaches a maximum of 2.8 µW at 51% of open-circuit voltage. Experimental results show that the tested hybrid harvesting system simultaneously generates 7.3 µW DC power, when the distance from the harvester to a 3 W EIRP 915 MHz transmitter is 5.5 m, and 1.8 µW DC power from a 1.8 *g* vibration acceleration peak.**

Keywords—Energy harvesting; wearable Devices; RF to DC converter; hybrid harvester; RF, vibration

I. INTRODUCTION

Energy harvesting is a process that converts different energy sources, such as solar, vibration, thermal, and RF energy, into electrical energy to power electronic devices. Energy harvesting and wireless power charging for wearable devices have recently become a focus of research. J. Bito et al. [1] developed a flexible wearable wristband with an embedded inkjet-printed RF antenna and doubler circuits to scavenge RF energy from a 1 W two-way talk radio signal. Another work [2] proposed a flexible wire converter integrated in a wearable wristband to wirelessly charge phones. A curved copper dipole antenna in the form of a wearable necklace to harvest RF power was discussed in [3], or wireless charging implantable devices [4] and [5] are inserted into human body. For biomechanical energy harvesting for wearable devices, A. Proto et al. [6] utilized a PVDF thin film covering around the knee to harness low frequency mechanical energy from human walking, while [7] inserted lead zirconate titanate (PZT) films into shoes to generate power from human walking pressure. However, most previous works have only considered using an individual energy harvesting source to power wearable devices. Because of the limited environmental energy available, one of the most important challenges in energy harvesting is designing energy-efficient transducers and low power conditioning circuits.

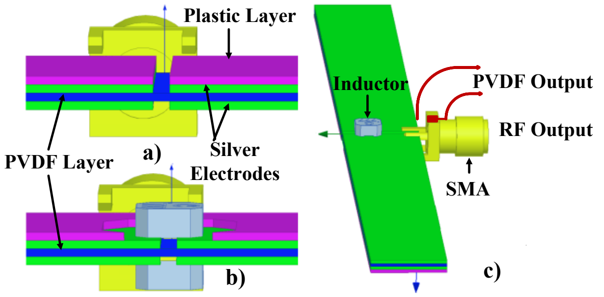

Fig. 1. Proposed hybrid harvester a) without and b) with inductor; c) side view.

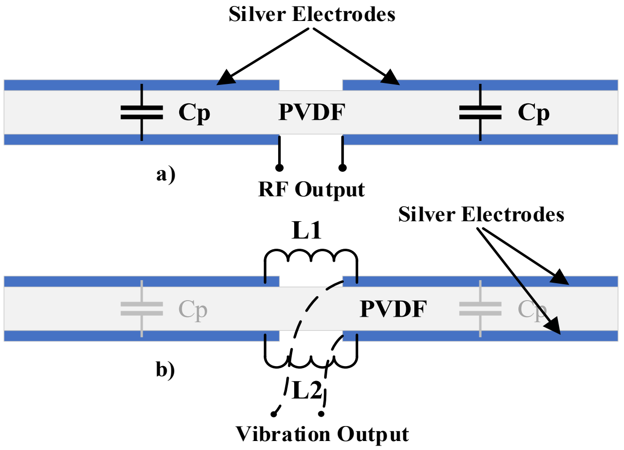

Fig. 2. a) Parasitic capacitors and b) added inductors (100µH-10mH) for hybrid energy harvester.

Recent research papers have focused on hybrid energy harvesters which simultaneously generate multiple outputs from different energy sources. For instance, Collado et al. [8] combined a solar cell and broadband copper antenna. In this paper, flexible antenna substrates and solar cell thin films provide a bending structure for the hybrid transducer. A similar research on wearable hybrid harvesting for smart fabric interactive textile was mentioned in [9]. The harvester which can be attached on human body obtains RF, solar and thermal energies. Another proposed hybrid harvester [10] which researched on triboelectric and electromagnetic achieves broadband and high output power. For vibration energy harvesting, a popular hybrid configuration [11] is using both piezoelectric and electromagnetic generators in which piezoelectric thin films were integrated in a cantilever, while the permanent magnets were attached at the beam tip.

978-1-5386-1180-7/18/$31.00 ©2018 IEEE

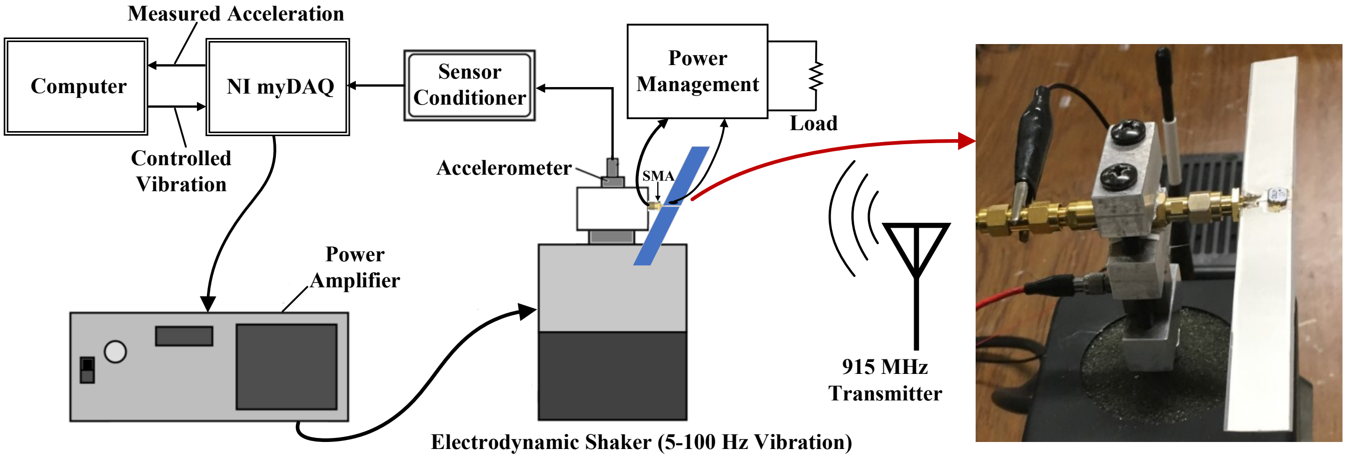

Fig. 3 The setup configuration of experimental measurements (left) and the fabricated hybrid energy harvester (right).

This paper proposes a solution to enhance energy harvesting for wearable devices by using a hybrid RF and vibration energy harvesting transducer. The silver electrodes of the hybrid harvester are used as a dipole antenna to harvest RF energy and combined with a PVDF thin film to form a sandwich structure to obtain vibration energy. The proposed energy harvester exploits the full size of the compact and flexible transducer without reducing harvesting efficiency and is flexible enough even to use as a necklace.

The proposed designs of the hybrid harvester with and without inductors are discussed in Section II. The transducer fabrication process and experimental evaluation of the hybrid harvesters is shown in Section III . Section III also describes the measured outputs of the hybrid harvesting systems with an RF to DC converter and AC to DC diode bridge rectifier are also presented. Finally, some conclusions are drawn in the last section.

II. HYBRID ENERGY HARVESTER DESIGN

The hybrid transducer illustrated in Fig. 1 and Fig. 2 consists of four layers: 2 silver electrodes, a middle PVDF layer and a polypropylene substrate. The top and bottom electrodes are etched into two left and right arms to form a dipole antenna. A female SMA connector is inserted at the middle of the thin film, connected to two top electrodes and used as a support for two cantilever vibration energy harvesters formed by the dipole antenna arms, one of which is shown in Fig. 3. The RF antenna of the harvester is designed for 915 MHz with the calculated length of

$$L = \frac{1}{2} A\lambda, \tag{1}$$

where A is the adjustment factor which depends on antenna thickness and width, and λ is the free space wavelength. Because of large parasitic capacitances created by the harvester's sandwich structure, at high frequency the top and bottom electrodes are shorted while the parasitic capacitance impedance, at low frequency, is sufficiently high that the bottom and top electrodes are isolated. Harvesting vibration energy requires using the top and bottom electrodes as the electrical output port of the hybrid transducer, while RF energy harvesting requires using the left and right pairs of electrodes as the output port. Connecting the cantilevers in parallel would short both arms of the dipole and degrade the RF harvesting performance. In this work, two vibration harvester configurations that avoid affecting the antenna performance were evaluated. In the first configuration, shown in Fig. 1.a) and Fig. 2.a), the cantilever that forms the ground electrode of the RF dipole is used to harvest vibration energy. The other cantilever, associated with the feedline of the RF dipole, was not employed. In the second configuration, shown in Fig 1.b) and Fig. 2.b), a connection between the two top electrodes and another connection between the two bottom electrodes are created at low frequency (e.g., 15 Hz) by using two inductors, each inductor connected in series with an electrode pair. At 915 MHz, the impedance of the inductors $Z_L = j\omega L$ becomes large enough that the inductors behave as RF chokes and have no significant effect on the antenna performance, and the hybrid transducer can utilize the whole transducer structure for harvesting both RF and vibration energy. An increase in power density in the constrained transducer volume is expected compared to the first configuration without inductors. The SMA connector attached at the middle of the thin film is the mounting point of the hybrid transducer. Ideally, a vibration will cause the transducer to deform symmetrically around the SMA connected point. By considering half of the thin film (a single cantilever) as a clamped-free beam as shown in Fig. 4, the vibration harvester can be represented as the mechanical equivalent mass-spring-damper system with a mass $m = m_{tip}$, a massless spring with total stiffness, and a damper with damping factor. The uniformly distributed mass along the thin film is equivalent to a tip mass

$$m = m_{tip} = \frac{33}{140} m_{film}. \tag{2}$$

The resonant frequency of the harvester can be derived from $\omega_o = \sqrt{k/m}$. The mechanical and electrical relationships [12] of the PVDF thin film are described as

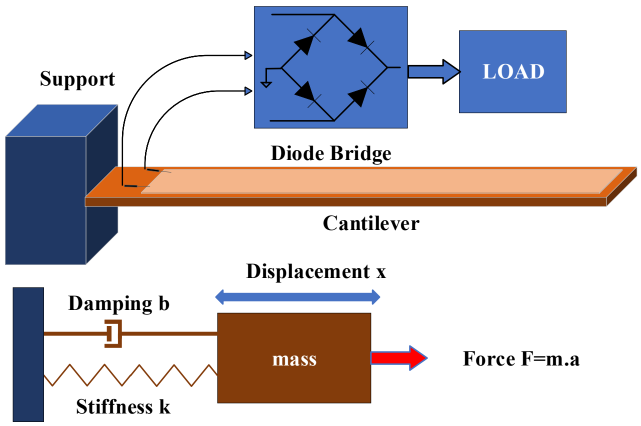

Fig. 4. Mass-spring-damper equivalent mechanical model of half of PVDF thin film.

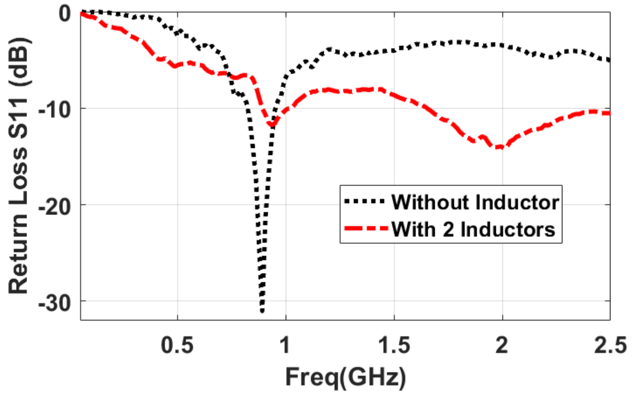

Fig. 5. Measured S11 for both transducer configurations versus frequency without vibration.

$$\begin{aligned} mx'' + bx' + kx + \alpha V &= ma \\ I + CV' &= \alpha x', \end{aligned} \tag{3}$$

where x, C, V, a and α are the mass displacement, output capacitance, output voltage, acceleration and force factor of the harvester, respectively. All empirical and calculating parameters of half of the hybrid harvester are shown in Table I.

III. EXPERIMENTAL RESULTS

Two 153 x 12 x 0.31 mm hybrid harvesters without and with inductors are shown in Fig. 3 and Fig. 11. The harvesters were fabricated from an A4 piezoelectric film sheet, 2-1004347-0 Piezo Film from TE Connectivity, which has a 52 µm thick PVDF layer and two silver ink top and bottom 6 µm thick electrodes. An SMA connector and 1 mH inductors (Coilcraft LPS4018-105MR) were mounted on the electrode surfaces of the harvester using low temperature silver epoxy. The test setup for the fabricated hybrid harvesters is also shown in Fig. 11. The RF output of the harvester was connected to a Keysight 8720C Network Analyzer to measure return loss S11 while the vibration harvester output was measured using an opamp-based buffer and a data acquisition device with Labview software. The hybrid harvester was mounted on a Labworks shaker ET-132 using an aluminum clamp. An accelerometer was also attached to the shaker to measure the vibration acceleration independently.

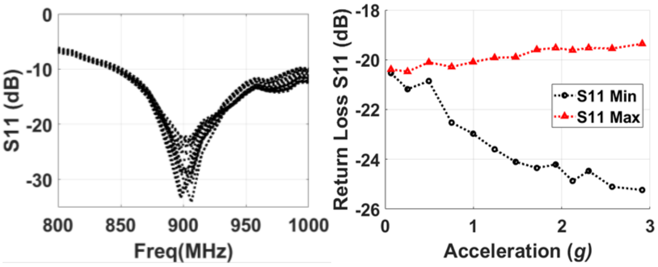

a) b)

Fig. 6. Measured S11 for transducer configurations a) versus frequency with 3 *g* vibration b) versus vibration acceleration at 915 MHz.

TABLE I. PARAMETERS FOR HALF OF HYBRID HARVESTER.

Symbol	Parameter	Value	Unit
m	Tip mass	$3.395\text{x}10^{-4}$	kg
k	Stiffness	3.16	N/m
LxWxT	Length x Width x Thickness	76.5x12x0.31	mm
C	Total capacitance	2.01	nF
f_o	Resonant frequency	15.1	Hz

Fig. 5. illustrates the measured S11 of the hybrid harvesters with and without inductors when no vibration was generated. The S11 of the harvester with inductors is -11.7 and -10.6 dB at 915 MHz and 2.4 GHz respectively. Inserting inductors into the hybrid harvester broadens RF harvesting bandwidth but increases S11 at 915 MHz. This tradeoff follows the well-known Bode-Fano Criterion. Another approach is using low-value inductors (which can be replaced by circular coils [13]) and parallel capacitors to achieve resonant frequency at 915 MHz. Fig. 6 a) and b) depicts the film vibration effects on antenna S11 with different frequencies and accelerations, respectively. In Fig. 7, the vibration output of harvesters with and without inductors has maximum power points at 6 MOhm and 3 Mohm respectively at the approximate resonant frequency of 15.1 Hz. The generated output power of the hybrid harvester with inductors is twice that from the harvester with no inductors. The maximum harvested vibration power before using a rectifier at the 3 *g* acceleration peak is 3.7 µW.

In this work, a 6-stage Dickson RF-to-DC converter (with an input matching network similar to [3] or [14]) and a diode bridge rectifier are connected to the RF and PVDF vibration harvester outputs, respectively. In Fig. 8 the output power of the RF-to-DC converter reaches a maximum at a resistive load from 18 kOhm to 22 kOhm when the input power from an RF signal generator is from -12 to -8 dBm.

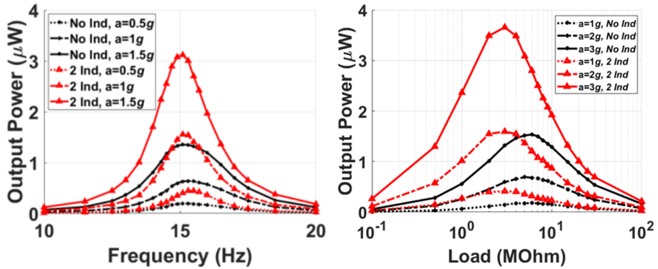

a) b)

Fig. 7. Measured output power versus a) frequency with different RMS accelerations and b) load resistance with different peak accelerations.

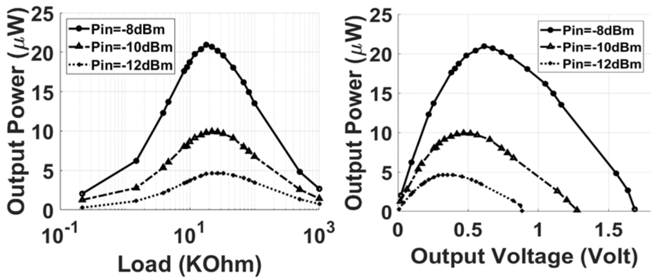

a) b)

Fig. 8. Measured RF-to-DC output power versus a) resistance load and b) output voltage.

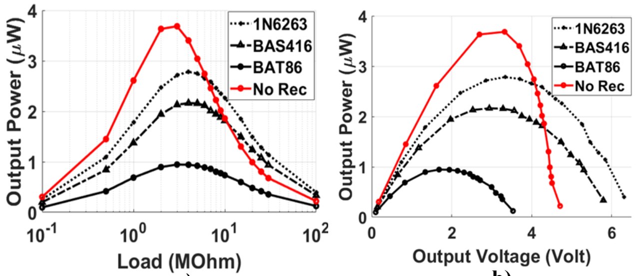

a) b)

Fig. 9. Measured AC-to-DC diode rectifier output power versus a) resistance load and b) output voltage.

Fig. 8b) shows that the output power reaches maximum at an output voltage from 36% to 40% of the open-circuit voltage. For vibration energy harvesting, the AC to DC rectifier using 1N6263 diodes shown in Fig. 9 obtains the highest power and reaches a maximum of 2.8 μW at a 4 MOhm resistive load. It is noteworthy that the output power with the rectifier is larger than that without the rectifier at high load resistance. This phenomenon was discussed and employed in [15] and [16] to significantly increase the output power by using a parallel switching inductor. The output maximum power points for the harvester with inductors after the rectifier circuit are around 50% of the open-circuit voltage in Fig. 9. The measured output power comparison between hybrid harvesters with and without inductors after using a rectifier is shown in Fig. 10. Finally, the whole hybrid energy harvesting system was simultaneously tested with a 3 W EIRP 915 MHz transmitter from Powercast and 15.1 Hz vibration with 1.8 *g* peak acceleration in Fig. 11. The measured transient response of the system is shown in Fig. 12. The transmitter was placed at a distance of 5.5 meters from the hybrid harvester in a typical office environment in Fig. 11.

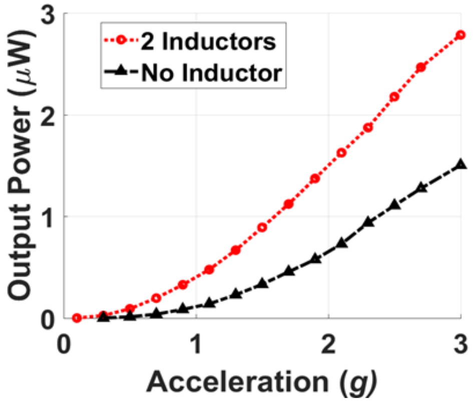

Fig. 10. Measured output power harvested from 15.1 Hz vibration versus acceleration of no inductor and 2 inductor harvesters.

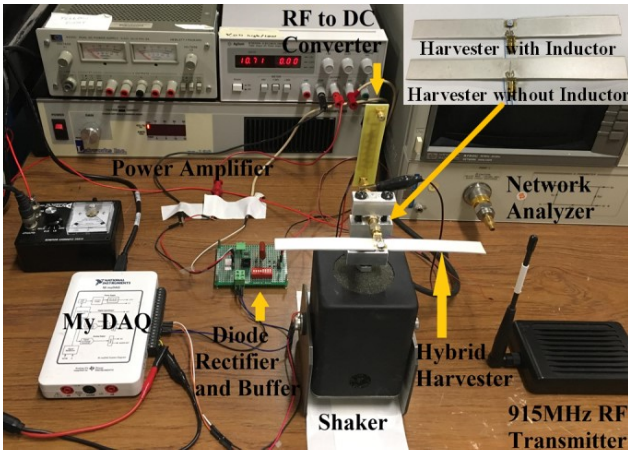

Fig. 11. Hybrid harvester system experimental setup.

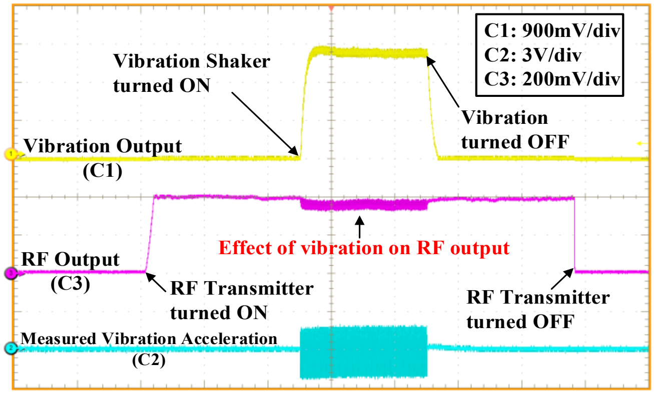

Fig. 12. Measured RF and vibration outputs of hybrid harvester.

The RF-to-DC converter output was connected to a 22 kOhm resistor and 10 uF capacitor while a half-wave rectifier was connected to a 3.3 MOhm resistor and 0.22 uF capacitor. This experiment shows that the fabricated hybrid harvester with inductors can simultaneously generate a 2.4 V output voltage with 1.8 μW DC power from vibration as well as a 0.4 V output voltage with 7.3 μW DC power from an RF signal.

IV. CONCLUSIONS

This work has shown a novel configuration of RF and vibration hybrid energy harvesting for wearable devices. A PVDF thin film is used to scavenge low frequency vibration energy, while an RF energy harvesting dipole antenna is fabricated from the silver ink electrodes of the film. An RF to DC converter and AC to DC rectifier are used to convert the harvester outputs to DC power. Future work will complete the hybrid harvesting system by designing a multiple-input buck and boost converter to provide power for a single load.

ACKNOWLEDGMENT

S. Nguyen was supported by Vietnam Education Foundation fellowship and a Google Faculty Research Award. The authors would like to thank R. Bhardwaj at Google-X for his feedback and support.

REFERENCES

[1] J. Bito, J. G. Hester and M. M. Tentzeris, "Ambient RF Energy Harvesting from A Two-Way Talk Radio for Flexible Wearable Wireless Sensor Devices Utilizing Inkjet Printing Technologies," IEEE Transactions on Microwave Theory and Techniques, vol. 63, no. 12, pp. 4533-4543, Dec. 2015.

[2] M. Tian, N. Wang, K. Wang, H. Jia, Z. Li, X. Yang and L. Wang "A wire-embedded converter used for wearable devices," 2017 IEEE Applied Power Electronics Conference and Exposition (APEC), Tampa, FL, 2017, pp. 121-125.

[3] S. H. Nguyen, N. Ellis and R. Amirtharajah, "Powering smart jewelry using an RF energy harvesting necklace," 2016 IEEE MTT-S International Microwave Symposium (IMS), San Francisco, CA, 2016, pp. 1-4.

[4] Y. Zou and S. O'Driscoll, "Implant Position Estimation Via Wireless Power Link," in IEEE Transactions on Circuits and Systems II: Express Briefs, vol. 62, no. 2, pp. 139-143, Feb. 2015.

[5] S. O'Driscoll et al., "A 200µm × 200µm × 100µm, 63nW, 2.4GHz injectable fully-monolithic wireless bio-sensing system," 2017 IEEE Radio Frequency Integrated Circuits Symposium (RFIC), Honolulu, HI, USA, 2017, pp. 256-259.

[6] A. Proto et al., "Wearable PVDF transducer for biomechanical energy harvesting and gait cycle detection," 2016 IEEE EMBS Conference on Biomedical Engineering and Sciences (IECBES), Kuala Lumpur, 2016, pp. 62-66.

[7] R. Meier, N. Kelly, O. Almog and P. Chiang, "A piezoelectric energy-harvesting shoe system for podiatric sensing," 2014 36th Annual International Conference of the IEEE Engineering in Medicine and Biology Society, Chicago, IL, 2014, pp. 622-625.

[8] A.Collado and A.Georgiadis, "Conformal Hybrid Solar and Electromagnetic (EM) Energy Harvesting Rectenna," in IEEE Transactions on Circuits and Systems I: Regular Papers, vol. 60, no. 8, pp. 2225-2234, Aug. 2013.

[9] S. Lemey, F. Declercq and H. Rogier, "Textile Antennas as Hybrid Energy-Harvesting Platforms," in Proceedings of the IEEE, vol. 102, no. 11, pp. 1833-1857, Nov. 2014.

[10] Kumar Gupta, Rahul & Shi, Qiongfeng & Dhakar, Lokesh & Wang, Tao & Heng, Chun-Huat & Lee, Chengkuo. (2017). Broadband Energy Harvester Using Non-linear Polymer Spring and Electromagnetic /Triboelectric Hybrid Mechanism. Scientific Reports. 7. 41396. 10.1038 /srep41396.

[11] A. Khaligh, P. Zeng and C. Zheng, "Kinetic Energy Harvesting Using Piezoelectric and Electromagnetic Technologies—State of the Art," in IEEE Transactions on Industrial Electronics, vol. 57, no. 3, pp. 850-860, March 2010.

[12] E. Lefeuvre, D. Audigier, C. Richard and D. Guyomar, "Buck-Boost Converter for Sensorless Power Optimization of Piezoelectric Energy Harvester," in IEEE Transactions on Power Electronics, vol. 22, no. 5, pp. 2018-2025, Sept. 2007.

[13] C. Van Pham, A. V. Pham and C. S. Gardner, "Development of Helical circular coils for wireless through-metal inductive power transfer," 2017 IEEE Wireless Power Transfer Conference (WPTC), Taipei, 2017, pp. 1-3.

[14] D. P. Nguyen, J. Curtis and A. V. Pham, "A Doherty Amplifier With Modified Load Modulation Scheme Based on Load-Pull Data," in IEEE Transactions on Microwave Theory and Techniques, vol. PP, no. 99, pp. 1-10.

[15] D. Guyomar, A. Badel, E. Lefeuvre and C. Richard, "Toward energy harvesting using active materials and conversion improvement by nonlinear processing," in IEEE Transactions on Ultrasonics, Ferroelectrics, and Frequency Control, vol. 52, no. 4, pp. 584-595, April 2005.

[16] Y. K. Ramadass and A. P. Chandrakasan, "An Efficient Piezoelectric Energy Harvesting Interface Circuit Using a Bias-Flip Rectifier and Shared Inductor," in IEEE Journal of Solid-State Circuits, vol. 45, no. 1, pp. 189-204, Jan. 2010.